Study of the phase transition in lysozyme crystals by Raman spectroscopy

Anna V. Frontzek (neé Svanidze)[1,2], Laurent Paccou[3], Yannick Guinet[3], Alain Hédoux[3]

[1] Jülich Center for Neutron Science (JCNS), Forschungszentrum Jülich GmbH, Outstation at MLZ, Lichtenbergstraße 1, 85747 Garching, Germany

[2] A.F. Ioffe Physical Technical Institute, Politekhnicheskaya ul. 26, 194021 St. Petersburg, Russian Federation

[3] Université Lille Nord de France, F-59000 Lille, France, USTL UMET UMR 8207, F-59655 Villeneuve d'Ascq Cedex, France

Corresponding author: A.V. Frontzek, e-mail: a.frontzek@fz-juelich.de

Abstract

Background: Recently, it has been revealed that tetragonal lysozyme crystals show a phase transition at 307 K upon heating. The underlying mechanisms of the phase transition are still not fully understood. Here we focus on the study of high-frequency vibrational modes arising from the protein and their temperature evolution in the vicinity of T_{ph} as well as on the detailed study of crystalline water dynamics near T_{ph}.

Methods: Raman experiments have been performed at temperatures 295-323 K including T_{ph}. The low-frequency modes and the modes of fingerprint region, CH- and OH-stretching regions have been analyzed.

Results and conclusions: In spite of the absence of noticeable rearrangements in protein structure, the high-frequency vibrational modes of lysozyme located in the fingerprint region have been found to exhibit the features of critical dynamics near T_{ph}. Pronounced changes in the dynamics of α-helixes and Tyr residues exposed on the protein surface point to the important role of H-bond rearrangements at the phase transition. Additionally the study of temperature evolution of OH-stretching modes has shown an increase in distortions of tetrahedral H-bond network of crystalline water above T_{ph}. These changes in water dynamics could play a crucial role in the mechanisms of the phase transition.

General significance: The present results shed light on the mechanisms of the phase transition in lysozyme crystals.

Keywords: phase transition, tetragonal lysozyme crystal, Raman spectroscopy

1. Introduction

All biochemical processes are accompanied by phase transformations in biopolymers. Therefore, changes in structure and dynamics of proteins and other biopolymers induced by interactions with ligands, variations in temperature *T*, pressure and other environmental conditions have been intensively studied in the past decades. Detailed information about the phase transitions in biopolymers can be inferred from studies of their crystalline state. Recently, it has been found that certain protein crystals exhibit phase transitions induced by dehydration [1,2] or temperature variation [3-5].

For the first time, a phase transition in protein crystals that occurs at temperature change was discussed by P. Jolles and J. Berthou [6]. They demonstrated that when tetragonal hen egg white lysozyme crystals with space group $P4_32_12$ are heated above 298 K in a mother solution, their symmetry becomes orthorhombic with space group $P2_12_12_1$ [6]. Later it was found that optical properties of tetragonal lysozyme crystals also change with increasing temperature [7]. In particular, Kobayashi et al. showed that the temperature dependence (*T*-dependence) of the birefringence index of lysozyme crystals exhibits a step-like anomaly near 306.5 K [7]. These data stimulated the recent interest in the investigation of lattice dynamics of tetragonal lysozyme crystals in the temperature region where a phase transition can occur by Brillouin light scattering [3,4] and calorimetry [4,5]. Brillouin light scattering experiments revealed anomalies in the *T*-dependences of velocity and integral intensity of the acoustic quasi-transverse phonon and in the velocity of the acoustic quasi-longitudinal phonon in the vicinity of 307 K. A similar behavior of acoustic phonons was observed earlier at phase transitions in ferroelectrics and ferroelastics [8]. This points to a critical lattice dynamics of lysozyme crystals which is a signature of the phase transition in them. The existence of phase transition in lysozyme crystals was also verified by ac-chip calorimetric measurements. It has been found that the *T*-dependence of heat capacity of the crystals exhibits λ-type anomaly in the vicinity of 303 K [4,5]. The comparative analysis of Brillouin scattering data [3,4] with the results of calorimetric [4,5] and optical [7] studies of lysozyme crystals gave a possibility to conclude that a structural phase transition indeed occurs in a tetragonal lysozyme crystal near 307 K (the phase transition temperature T_{ph}). However, the nature of this phase transition is still unclear.

In this work we applied Raman spectroscopy in the vicinity of T_{ph} in order to shed light on particular changes in protein dynamics and dynamics of crystalline water forming

tetragonal lysozyme crystals. The principle of Raman scattering is best described in numerous monographs [9-13]. Although the principle of "Raman effect" was discovered in crystals by L.I. Mandelstam and G.S. Landsberg and independently by C.V. Raman and K.S. Krishnan in liquids in 1928, its practical applications have been realized only after development of appropriate laser sources and powerful computer technology for data analysis. Now, Raman spectroscopy is widely used for determination and investigation of high-frequency excitations in vibrational spectrum of various kinds of materials – from inorganic [14] and organic with crystalline, glassy and liquid states [11,15] up to biopolymers [17-20], food [13] or biological tissues [21,22]. The method is non-invasive and non-destructive and, therefore, perfectly suited for the investigation of such fragile and sensitive objects as protein crystals. Recent Raman scattering studies of tetragonal lysozyme crystals were devoted to the low-frequency part of Raman spectra including the contributions of relaxation components and vibrational modes and its evolution induced by changes in content of crystalline water [18]. The analysis of the fingerprint region in high-frequency Raman spectra of lysozyme crystals gave a possibility to identify vibrational modes of some structural elements of protein macromolecule [19,20]. However, the effect of temperature on the crystals has been investigated mainly in connection with the problem of protein denaturation within the crystalline environment [19].

A specific feature of all protein crystals is that they contain a considerable amount of water which fills in the space between regularly arranged protein molecules forming the crystals. Tetragonal lysozyme crystals considered in the present work contain up to 46% of water [23]. Recently, it has been demonstrated that dehydration itself can induce a structural phase transition in protein crystals. In particular, dehydration of monoclinic lysozyme crystals can lead to the structural phase transition accompanied by conformational rearrangements of the protein main chain in the region Gly71-Asn74, a suppression of protein rigid body motions and a dehydration-induced increase in number of intermolecular contacts [1]. Tetragonal lysozyme crystals have been also revealed to show a structural phase transition at dehydration for ~ 88% relative humidity which manifests itself not only as introduction of additional disorder in the crystal structure, but also as a discontinuity and hysteresis of the lattice parameter c [2]. Therefore, the first question accompanying any discussions about phase transitions in protein crystals concerns a role of water and changes in water content and dynamics in crystals which could occur at a phase transition.

The purpose of present work was to investigate the dynamics of (i) crystalline water and (ii) protein molecules forming lysozyme crystals in the vicinity of the phase

transition that occurs at crystal heating. i) To scan the temperature behavior of relaxational dynamics and vibrational modes of water in the crystal, we have performed Raman scattering experiments in two frequency ranges. These regions, 10-400 cm^{-1} and 2600-4000 cm^{-1}, were chosen because of the following reasons: the first one has been previously demonstrated to exhibit relaxation component due to the water relaxational motions [18]; it has been also shown to contain the vibrational modes which are influenced by the dynamics of bulk water and water of hydration shell [24]; the second region includes bands of OH-group stretching vibrations. ii) The information regarding the high-frequency vibrational modes localized on some certain atomic groups of protein molecules has been obtained in detailed study of the fingerprint region of lysozyme crystal Raman spectra. Raman measurements with increasing temperatures were performed also in frequency region of CH-stretching vibrations in order to estimate if the fast dynamics of CH, CH_2 and CH_3 groups belonging to the protein undergo any changes at the phase transition.

2. Materials and methods

2.1 Materials

Hen egg-white lysozyme purchased from Fluka has been used for crystal growth without further purification. Tetragonal lysozyme crystals with space group $P4_32_12$ were grown by "hanging drop vapor diffusion" method at temperature ~22°C [25]. The reservoir contained 6 % (w/v) sodium chloride dissolved in 0.1 M sodium acetate buffer, pH 4.6. Protein crystals grew in the drop containing the mixture of 6 µl reservoir solution and 6 µl 5% (w/v) protein solution prepared in the same buffer. Sodium azide was added into the solution where the crystals were grown to prevent bacterial contamination. In order to perform each Raman scattering experiment we used one single lysozyme crystal with plate-like shape [25] packed in the glass capillary with some amount of solution where the crystal was grown. It was done to avoid water evaporation form the crystal. The crystals with the sizes of about $0.3\times0.3\times0.5$ mm^3 were chosen for Raman experiments.

2.2 Raman scattering experiment

Raman spectra have been recorded by two different spectrometers that gave a possibility to investigate different frequency ranges. The first experimental setup which allows exploring the low-frequency domain down to 7 cm^{-1} consists of Argon-Krypton Coherent laser

(wavelength λ=514.5 nm) used as an excitation source, XY Dilor spectrometer and CCD camera for data accumulation. The Raman spectrometer includes a double monochromator grating dispersion system composed of four mirrors with a long focal length coupled to an additional grating system of the spectrometer. Keeping the entrance, intermediate and exit slits opened at ~ 150 μm allows high rejection of the elastic scattered light. These experimental conditions lead to a resolution less than 1.5 cm^{-1} for the 514.5 nm incident light. The capillary with the lysozyme crystal was mounted in the goniometer in front of incoming regulated nitrogen-flow from the Oxford device for temperature control. The sample has been heated gradually from 293 K up to 320 K with the accuracy of temperature maintenance of ~ 0.5. The incident laser beam was directed into the crystals on the other side of the crystals and Raman spectra were collected in backscattering geometry.

Since anisotropy is an intrinsic property of any crystals including tetragonal lysozyme crystals, Raman spectra are dependent on crystal orientation with respect to the wave-vector of incident and scattered light and polarizations of their electric fields [9,10]. Unfortunately, it was not possible to obtain polarized low-frequency Raman spectra of lysozyme crystals as well as to mount the single crystal under the microscope for appropriate crystal axis orientation because of strong loss in signal intensity. Therefore, in order to follow the temperature evolution of Raman spectra associated with the changes in the dynamics of crystal lattice and exclude the influence of crystal reorientation, the same single crystal with a fixed orientation was measured during the whole experiment.

In order to measure Raman spectra at frequencies higher than 400 cm^{-1} Renishaw InVia Raman microspectrometer consisting of a single-grating spectrograph coupled to an optical Leica microscope was used. The excitation sources with different wavelengths could be chosen depending on the frequency range investigated. A red laser (λ= 785 nm) was used to scan a frequency range of 400-1850 cm^{-1} whereas a Coherent Argon laser with λ=514.5 nm – to probe CH and OH stretching vibrations at frequencies 2800-4000 cm^{-1}. The experiments with different laser sources have been performed separately with two different lysozyme crystals having similar shape and sizes. Each crystal packed into the glass capillary was placed under the 50X long-working distance objective, directly on the metallic surface of microscope goniometer with temperature control. The temperature of the crystal was increased from 295 K up to 323 K stepwise and maintained with the accuracy of 0.1 K during the experiment by a THMS 600 Linkam temperature controller. The crystal was kept 10 min. at each temperature point before spectrum recording. The grease “no name” between capillary and metallic surface

facilitated thermal conductivity. The use of the microscope allowed focusing of incident light in the volume of ~ 150 μm^3 inside the lysozyme crystal and an appropriate orientation of the crystals with respect to the incident light.

For crystal materials the number of Raman active-modes that can be detected by Raman spectroscopy mainly depends on the crystal symmetry, scattering geometry and polarizations of incident and scattered light. In our Raman experiments performed in frequency ranges 400-1850 cm^{-1} and 2800-4000 cm^{-1} the laser light was vertically polarized and directed perpendicular to the plate (110) of lysozyme crystal, the scattered light was collected in back-scattering geometry as it is shown in Fig. 1. The polarization of scattered light was not registered (an analyzer was not used). Since the crystal rotates the polarization of laser light, the electric field of the light scattered in the crystal can be decomposed to the projections on the axes x and z. Thus, the scattered light could be considered as a superposition of xz (crossed polarizations of the incident and scattered radiations) and zz polarization (parallel polarizations of the incident and scattered radiations) geometries. The polarized Raman experiment performed for frequency range 400-1800 cm^{-1} with the same crystal orientation demonstrated the presence of strongly polarized, strongly depolarized and partially depolarized Raman lines [20]. The overwhelming majority of all Raman active-modes in the frequency range 400-1850 cm^{-1} (fingerprint region) manifests itself in case of zz geometry and, therefore, can be observed in our experiment. In contrast to fingerprint region, it was proven by Raman measurements performed at different polarizations that vibrational bands of C–H, N–H and O–H groups observed in high-frequency region 2600-4000 cm^{-1} don't depend on the polarization [20]. It is explained by the fact that there exist a vast amount of randomly oriented C–H, N–H and O–H groups in any protein crystal.

Since the bands in recorded Raman spectra had a very well distinct shape, the standard fitting procedure using Gaussians and Lorentzians has been performed. PeakFit v4.12 (Systat Software Inc. [26]) was used to fit the spectra. The molecular graphic program CCP4MG version 2.9.0 was utilized to plot lysozyme molecule and mark amino acid residues in it.

The low-frequency Raman scattering data for dry lysozyme powder and 20% aqueous lysozyme solution were taken from paper of A. Hédoux et al. [24]. The high-frequency Raman spectra in the range of OH-stretching bands for water [27] and dry lysozyme [28] were taken from previous studies.

3. Results and Discussions

3.1 High-frequency vibrational modes of lysozyme and their behavior in the vicinity of T_{ph}

3.1.1 Fingerprint region of Raman spectra (400-1850 cm^{-1})

The Raman spectra analysis in the fingerprint region can provide information about vibrations of aromatic amino-acid residues and disulfide bonds as well as the dynamics of protein secondary structure based on amide I and amide III bands and modes related to polypeptide backbone. Fig. 2 shows Raman spectra of the tetragonal lysozyme single crystal with the assignment of some bands to the vibrations of certain structural elements of lysozyme molecule. The interpretation of peaks was made according to the previous investigations of monoclinic and tetragonal lysozyme crystals [19,20], lysozyme solution [29] and hydrated powder [17]. The list of bands considered in the present work and their respective interpretation are summarized in Table 1.

The fingerprint region in Raman spectra of lysozyme crystal measured at different temperatures is shown in Fig. 2. It can be seen that the Raman intensity of light scattering in the crystal drops significantly with increasing temperature above 304 K. According to the fluctuation-dissipation theorem, the spectral function $S(\omega)$ is proportional to the imaginary part of susceptibility $\chi''(\omega)$ [4,30]. Thus, the integral intensity of vibrational modes is proportional to the static real part of the susceptibility $\chi'(0)$. Therefore, the drop in integral intensity can be explained by the change of the susceptibility at the phase transition. In the temperature interval from 304 K up to 310 K a further sharp decrease in intensity of Raman spectra is observed, while the intensity starts to increase again above 313 K accompanied with the reconstruction of the previous spectrum quality. An example of the changes in integral intensity as function of temperature is given in insert in Fig. 2 showing the intensity of Trp band located at 759 cm^{-1}. This temperature behavior can be generalized to all other bands of the spectrum. The first anomaly in T-dependence of intensity is assigned to the phase transition in the crystal. The mean temperature of this anomaly (~307 K) is the same as T_{ph} found in Brillouin light scattering and calorimetric experiments [3-5]. We associate the following rise in intensity with crystal dehydration. This conclusion has been made based on the detailed study of water dynamics in lysozyme crystals by Raman

scattering at low frequencies and at frequencies of OH-stretching region (the data are presented in Section 3.2). Dehydration of the crystal used for the study of fingerprint region occurred above 314 K; the crystal used for studying of CH stretching region showed first signs of losing crystalline water above 319 K.

In order to clarify which modes are affected by the phase transition, the temperature evolution of Raman bands corresponding to some selected vibrational modes have been investigated.

3.1.1.1 Secondary structure of polypeptide backbone

Amide-I band. The amide-I band is mainly associated with C=O stretching vibrations (~80%) and some additional contributions from N–H bending and C–N stretching vibrations as well as C–C–N deformations [17,29]. The position of the amide-I peak in Raman spectra depends on the strength of hydrogen bonds formed by dipole-dipole interactions between C=O and N–H groups of amide. An inherent difference in strength of hydrogen bonding in α-helical structures, β-sheets, β-turns and other structural elements leads to the variation of frequency of the amide-I band depending on secondary structure content of a protein. Therefore, the analysis of the amide-I band's temperature behavior in the vicinity of T_{ph} gives a possibility to conclude if the phase transition is accompanied by changes in secondary structure of lysozyme molecule.

In the spectra of tetragonal lysozyme crystal, the amide-I band is clearly observable at 1659 cm^{-1} (Fig. 3a). It is assumed to be sensitive to the conformation of α-helical secondary structure of polypeptide chain and is frequently used to determine changes in α-helix content or strength of hydrogen bonding [31]. The native structure of hen egg-white lysozyme contains a relatively big amount of α-helical structures (40-42%) which are organized in four α-helixes stabilizing the α-domain [32]. Their vibrational motions give a significant contribution to the Raman spectra. The *T*-dependences of Raman frequency and width of the amide-I band obtained for the lysozyme crystal (Fig. 3b) exhibit pronounced anomalies: (i) the band undergoes slight downshift near 306 K and then an upshift back to its original position at further crystal heating above 314 K; (ii) the width of the band sharply increases in the vicinity of 306 K, but above ~ 314 K the peak narrows again. The anomalies near 306 K are evidence of the phase transition in the crystal while the changes at 314 K are supposed to be due to crystal dehydration. The amide-I frequency downshift near T_{ph} indicates the compression and strengthening of hydrogen bonds in α-helixes of lysozyme molecules. Such a relation between frequency shift of the amide-I band and changes in H-bond network was demonstrated in a

study of lysozyme denaturation upon pressurizing [28]. It was found that the pressure increase in lysozyme solution induces a decrease in frequency of CO stretching bands involved in CO···H hydrogen bonding [28]. The broadening of the amide-I band at the phase transition points to structural disorder on the local level. We don't attribute any observed anomalies in the amide-I temperature behavior to the unfolding of α-helixes because the thermal denaturation of lysozyme occurs at temperatures around 343 K and the usual distortion of the amide-I band-shape associated with the secondary structure unfolding is not observed in the present work [24,33].

Amide-III band. The amide-III band originates mainly from the N-H bending and the C–N stretching vibrations and includes a small contribution from C=O in-plane bending and C–C stretching vibrations [31]. It is extremely sensitive to the changes in protein backbone conformations and can be associated with different types of secondary structure depending on the frequency range where it appears. In the Raman spectra of lysozyme tetragonal crystal amide-III bands were identified at 1235 cm^{-1} and 1259 cm^{-1} (Fig. 3c) which correspond to β-sheet and disordered structures, correspondingly. These are the only bands in fingerprint region of lysozyme crystal Raman spectra which shift towards higher frequencies (for ~2 cm^{-1}) above 306 K (Fig. 3d). Further heating of the crystals above ~314 K is accompanied by a downshift of the bands back to the frequencies recorded at room temperatures. In spite of the fact that the peaks look broadened above T_{ph} because of the extreme decrease in intensity (Fig. 2), the *T*-dependences of widths of both bands are smooth and don't exhibit any anomalies in the vicinity of T_{ph} (data are not shown). Usually an upshift of a mode is theoretically interpreted to be due to more dense packing and bond strengthening [34]. However, it could be different in case of NH···O hydrogen bonding [28].

N-C_α-C main-chain vibrations. The bands with maximums located at 899 cm^{-1} and 932 cm^{-1} are associated with the stretching vibrations of N-C_α-C of protein main chain (Fig. 3e) [17,31]. The both bands correspond to the vibrations in α-helixes. Crystal heating above the phase transition (~306 K) is accompanied by the slight downshifts of the bands (Fig. 3f) that can be due to a compression of α-helical structures in the high-temperature phase [28]. Such a behavior agrees well with temperature evolution of the amide-I band which points to the strengthening of hydrogen bonds in α-helixes above T_{ph}.

3.1.1.2 Raman markers corresponding to side group vibrations

The most pronounced bands observed in the Raman spectra of proteins are arising from the vibrations of aromatic side chain groups and disulfide bonds [31]. Lysozyme contains all five

varieties of aromatic groups [32], but contributions of only three of them are visible in Raman spectra of tetragonal lysozyme crystals (Fig. 2). In particular, the vibrations of Trp are distinguishable as bands at 759, 875, 1010, 1336, 1361, 1552 and 1579 cm^{-1}, Tyr modes can be identified at 835, 858, 1176, 1194, 1209 and 1613 cm^{-1} and Phe bands manifest themselves at 621, 1003 (the most intensive characteristic band of Phe) and 1209 cm^{-1}. In addition, the bands of Met side groups (695 and 721 cm^{-1}) and disulfide bridges (507 and 525 cm^{-1}) can be identified in spectra of lysozyme crystals [19,20,29,31]. It is seen in Fig. 2 that intensity of light scattered in lysozyme crystal drops significantly when the temperature is approaching T_{ph}. As a consequence it becomes complicated to analyze the temperature evolution of some Raman peaks in high-temperature phase. Only the vibrational modes with clearly defined T-dependences of Raman shift and bandwidth in the whole investigated temperature range are considered here.

Trp bands. The polypeptide chain of hen egg-white lysozyme contains six tryptophan residues [32]. They are localized in positions 28, 62, 63, 108, 111 and 123 of protein primary structure (Fig. 4, insert). Trp-62 and Trp-63 lie in the active-site cleft of lysozyme molecule from the side of β-domain while Trp-108 contributes to the surface of the active-site cleft from the side of α-domain. The indole ring of Trp-123 lies roughly parallel to the surface of protein molecule, partly shielding Cys-30 from the contact with surrounding liquid [32]. All four mentioned Trp residues are exposed to the solvent and can participate in the formation of hydrogen bonds with the water of primary hydration shell. Contrary to them Trp-28 and Trp-111 are buried into the hydrophobic interior. Raman bands of Trp residues are sensitive to the changes in hydrophobicity of indole ring environment, hydrogen bonding, Trp conformations and cation-π interactions [35].

The commonly accepted indicator for hydrophobic/hydrophilic environment of tryptophan indole ring for proteins in solvent is also relative intensity of Fermi doublet (vibrational mode W7) at 1360 and 1340 cm^{-1}. For the tetragonal lysozyme crystal the doublet was identified in Raman spectra at 1336 and 1361 cm^{-1}. It originates from Fermi resonance between a fundamental band of in-plane $N_1=C_8$ vibration of indole ring and one or more combination bands of out of plane vibrations [17,31]. If the relative intensity of the Fermi doublet I_{1361}/I_{1336} is smaller then 1, a tryptophan is assumed to be in hydrophilic environment or exposed to aqueous solution. And opposite, if the ratio is larger than 1, it is surrounded by hydrophobic environment, for example, is situated in the protein hydrophobic core [31]. For tetragonal lysozyme crystals the ratio of intensities I_{1361}/I_{1336} at room temperature is ~ 0.12-0.18 that is

explained by the fact that the four of six Trp residues of lysozyme molecule are exposed to water hydration shell. The variation of I_{1361}/I_{1336} value in the vicinity of T_{ph} is diminutive that is an evidence of stable positioning of Trp residues and absence of any changes in hydrophobicity of the Trp microenvironment upon heating.

The other Trp marker is W3 mode with the frequency near 1552 cm^{-1} (Fig. 3a). It arises from the $C_2=C_3$ stretching vibrations of indole ring and is usually used as a conformation marker because the peak position is sensitive to the changes of the torsion angle ($\chi^{2,1}$) about the $C_2=C_3–C_\beta–C_\alpha$ linkage [35]. Our experimental results show that the position of the band remains the same over the whole temperature interval while the bandwidth gets broader upon heating above 307 K (Fig. 4). The broadening of the band is consistent with the view that vibrations of indole rings become more disordered above T_{ph}. It either can be a result of increased fluctuations around the $C_2=C_3–C_\beta–C_\alpha$ linkage of some or all six Trp residues.

Tyr bands. Lysozyme contains tree tyrosine residues, in particular, Tyr-20, Tyr-23 and Tyr-53 (Fig. 5, insert) [32]. The first two are situated in helical domain while the third is in β-domain. All tyrosine residues are located close to the surface of lysozyme molecule.

Only one band of Tyr residues exhibits well defined temperature dependence (Fig. 5). It locates at 1613 cm^{-1} (mode Y8a; an example of spectrum fitting in the frequency range of the band is shown in Fig. 2a) and originates from the C-C stretching vibrations within the aromatic ring [31]. The frequency of 1613 cm^{-1} Tyr band decreases above T_{ph} = 307 K. The downshift of the band can be due to changes of hydrogen bond strength between Tyr and water of primary hydrogen shell. This shows close relationship between rearrangements in water and protein dynamics.

C-S Stretching band. Lysozyme contains two Met residues (Met-12 and Met-105) buried in hydrophobic core of protein molecule (Fig. 6a, insert). The Met band can be identified in Raman spectra of lysozyme crystal at 694 cm^{-1} (Fig. 6a). This mode originates from C–S stretching vibrations of $–S–CH_2–CH_2–$group conformer in gauche conformation obtained by rotation around $–S–CH_2–$ bond [17]. It can be seen in Fig. 6b that the Raman shift of the band undergoes a subtle downshift above T_{ph}=307 K while the width distinctly narrows near the same temperature. The variation in the band frequency points out to the local conformational changes near Met residues which might lead to an additional extension of C–S stretching vibrations. Since the width of the band gets narrow in the vicinity of the phase transition, most probably the conformational rearrangements lead to the ordering of Met group vibrations.

Bands of disulfide bonds. The three-dimensional structure of lysozyme is stabilized by 4 disulfide bridges [32]. Three of them, Cys6-Cys127, Cys30-Cys115 and Cys64-Cys80, have a gauche-gauche-gauche (ggg) conformation. Their vibrations give rise to the strong line at 507 cm^{-1} in the Raman spectra of lysozyme crystal. The 506 cm^{-1} band can be characterized in whole investigated temperature range. The T-dependences of its frequency and bandwidth exhibit anomalies near 307 K. In particular, the band gets broader and shifts to lower frequencies with increasing temperature demonstrating an additional disordering and stretched vibrational motions above T_{ph} (data are not shown).

3.1.2 CH stretching region (2800-3100 cm^{-1})

Lysozyme like other proteins exhibits CH stretching vibrational bands in the 2800-3100 cm^{-1} frequency region of Raman spectrum. They originate from fundamental CH stretching vibrations, Fermi resonance between different CH stretching vibrations or their overtones [36-38]. The discrete bands observed in CH region can be assigned to symmetric and asymmetric vibrations of methyl CH_2, methylene CH_3 groups and to =C-H groups of unsaturated and aromatic amino acid residues [38]. Since methyl and methylene groups are distributed over whole protein molecule, variations in parameters of corresponding bands provide information about general features of fast protein dynamics, and hydrophobic core of protein, in particular. Beside protein molecules, lysozyme crystals include CH_3 groups of acetic acid and sodium acetate used to prepare sodium acetate buffer for lysozyme crystal growth. However, CH stretching bands of both these compounds are present in Raman spectra at frequencies different than protein CH stretching bands and, consequently, don't affect the analysis of C-H region of protein Raman spectra [16,39,40].

The CH region of lysozyme crystal Raman spectra contains five well-resolved bands located at 2875 cm^{-1}, 2907 cm^{-1}, 2933 cm^{-1}, 2964 cm^{-1} and 3059 cm^{-1} (Fig. 7). The most probable assignment of the bands to vibrations of protein groups were made on the basis of literature. We ascribe the 2876 cm^{-1} and 2964 cm^{-1} bands to symmetric and asymmetric stretching vibrations of CH_3 groups [38], the bands at 2907 cm^{-1} and 2933 cm^{-1} – to symmetric and asymmetric stretching vibrations of CH_2 groups, respectively [11,21,38], and the 3059 cm^{-1} band – to =C-H stretching vibration of aromatic residues [11,38]. It is necessary to note that interpretation of CH stretching bands of proteins is not a straightforward task: such complex substances as proteins contain a vast amount of CH groups belonging to different amino acid residues and

exposed to different microenvironment that leads to overlapping and broadening of some bands. As a result, Raman spectra of monomers in liquid or solid states could differ strongly from spectra of polypeptide chains. Therefore, there exist still some contradictions in peak assignment. For example, the main CH band at 2933 cm^{-1} observed in Raman spectra of various proteins is also attributed to totally symmetric stretching vibration of CH_3 functional groups [11,20]; the bands at 2875 cm^{-1} and 2964 cm^{-1} might include contributions from R_3CH and α-CH stretching vibrations, correspondingly [38].

The analysis of lysozyme crystal Raman spectra measured upon crystal heating from 294 up to 330 K allowed to plot *T*-dependences of frequencies and bandwidths (half-width at half-maximum (HWHM)) of all bands present in CH region. The data for four bands are shown in Fig. 8. It is clearly seen that all of them exhibit pronounced anomalies near 305 K which are due to the phase transition in the lysozyme crystal. Structural phase transitions in inorganic materials are accompanied by temperature behavior of optical phonons similar to the behavior of CH-stretching modes of lysozyme crystals [14].

In the following we consider in more detail which particular changes occur with CH modes in the lysozyme crystal under heating. As can be seen in Fig. 8, frequencies and bandwidths of bands located at CH region of lysozyme crystal Raman spectra vary with temperature quite differently. The phase transition is accompanied, on one hand, by ordering of symmetric CH_3 stretching vibrations and disordering of asymmetric one that can be concluded from the corresponding changes in bandwidth of 2876 and 2964 cm^{-1} bands, respectively, and, on the other hand, by disorder of symmetric CH_2 vibrations and ordering of asymmetric as evidenced through the broadening and narrowing of 2906 and 2932 cm^{-1} bands above 305 K. Such opposite changes in bandwidths of symmetric and asymmetric bands encourage the idea that an interaction between those vibrational modes might exist: disordering in one type of vibrations is associated by ordering of the other one. The frequencies of the both CH_3 vibrational modes decrease in values above T_{ph} whereas CH_2 stretching modes exhibit the opposite behavior – their frequencies increase above T_{ph}. The temperature evolution of the 3059 cm^{-1} band arising from stretching of =C-H groups of aromatic side chains is not shown. It was difficult to make a conclusion regarding the frequency changes as a function of temperature for this band due to big error bars. However, the bandwidth of 3059 cm^{-1} band demonstrates the T-dependence similar to $\nu_{as}(CH_3)$ and $\nu_{sym}(CH_2)$ modes.

3.2 Dynamics of crystalline water

3.2.1 Low-frequency Raman studies (10-400 cm^{-1})

An example of low-frequency Raman spectrum of lysozyme crystal measured at 295 K and the results of its fitting are depicted in Fig. 9a. It looks similar to the spectra presented by Urabe et al. for similar tetragonal lysozyme crystals obtained in polarized Raman scattering experiment [18]. In spite of strict ordering in arrangement of protein molecules in crystal structures, the low-frequency Raman spectra of the crystal resemble the spectra of disordered systems [12,28]: they include overlapping contributions of quasi-elastic scattering (QES) and vibrational modes (Fig. 9a). This can be explained by the presence of water in the crystal which facilitates protein dynamics playing a role of plasticizer, on one hand, and exhibits the features of its own dynamics in Raman spectra, on the other hand.

So, the spectrum presented in Fig. 9a contains a clearly distinguishable QES appearing due to the relaxational motion of crystal water [18] and peaks corresponding to low-frequency vibrational modes. The relaxation component was fitted by a Lorentzian centered at 0 cm^{-1}, while for the vibrational modes log-normal distributions and Gaussians were used.

In order to analyze the temperature behavior of low-frequency vibrational modes we first subtracted the QES contribution from the reduced Raman intensity $I_r(\omega)$ and then the reduced intensity was transformed to the imaginary part of dynamic susceptibility $\chi''(\omega)$ using the equations:

$$I_r(\omega) = \frac{I(\omega)}{B(\omega)\,\omega} \tag{1}$$

$$\chi''(\omega) = I_r(\omega)\,\omega \tag{2}$$

$$B(\omega) = n(\omega) + 1 \quad , \; n(\omega) = \left[\exp\left(h\omega/kT\right) - 1\right]^{-1} \tag{3}$$

where $I(\omega)$ is an observed Raman intensity, $B(\omega)$ and $n(\omega)$ are the temperature and Bose factors, respectively [12,18,24,28]. The dynamic susceptibility $\chi''(\omega)$ obtained from the Raman spectrum of lysozyme crystal shown in Fig. 9a by the described procedure is represented in Fig. 9b. Again, log-normal distributions and Gaussians were used for fitting the peaks corresponding to the vibrational modes.

The comparison of $\chi''(\omega)$ of lysozyme crystal with $\chi''(\omega)$ of dry lysozyme and lysozyme solution allowed us to identify low-frequency modes of lysozyme crystal

originating purely from protein dynamics and modes which are induced or influenced by presents of water in the system. Fig. 10 shows those $\chi''(\omega)$ of all mentioned systems obtained at room temperature T_{room} and a spectrum of lysozyme crystal recorded at elevated temperature of 310 K. The common feature of all the spectra is a presence of intensive vibrational mode at ~ 70 cm^{-1} assigned to the protein dynamics [24,28,41]. It has been previously observed also in Raman spectra of different proteins in dry state and protein solutions [24,28,41]. In the case of lysozyme crystal and lysozyme solution the low-frequency side of the band associated with protein dynamics is broader than in case of dry lysozyme, in other words - it features a shoulder around 50 cm^{-1}. Since the band at ~ 50 cm^{-1} is present in Raman spectra of pure water and its nature has generally be explained by the caging effect [42,43], it could be assumed that the band at ~ 50 cm^{-1} in $\chi''(\omega)$ of lysozyme crystal reflects a water-protein interaction. It is also worth noting that this band's intensity increases during lysozyme thermal denaturation which was interpreted to be due to water penetration into the protein interior [24]. The spectrum of the lysozyme aqueous solution in Fig. 10 differs from others by the broad hump around 170-180 cm^{-1}. It originates from intermolecular OH stretching vibrations in bulk water [42,43]. An additional increase in intensity in the spectrum of lysozyme crystal with respect to the spectrum of dry lysozyme in the 150-230 cm^{-1} frequency range is likely associated with the contribution of collective vibrations of water molecules in the H-bond network of bulk water filling in the space between lysozyme molecules.

The comparison of lysozyme crystal low-frequency Raman spectra measured at T_{room} and after heating up to 310 K (Fig. 10) gave the possibility to reveal some features of vibrational modes temperature evolution that could be due to the phase transition. In particular, the temperature increase above T_{ph} leads to a change in frequency of the band associated with protein dynamics. The T-dependence of frequency maximum of the band located at ~ 70 cm^{-1} is plotted in Fig. 11. It exhibits monotonic behavior with gradually increasing frequency and a kink at ~ 303 K, the temperature close to the presumable temperature of the phase transition in compliance with previous Brillouin light scattering and calorimetric experiments [3-5]. Above 303 K the T-dependence of the frequency continues to show a gradual increase but less steep than below T_{ph}. In general, the hardening of the vibrational mode seems to be very unusual behavior upon heating. It could be therefore assumed that the protein dynamics are affected by the changes in the surrounding water.

The spectra at elevated temperature also feature a slight variation in intensity in the range 150-230 cm^{-1}. An appropriate fit of 150-230 cm^{-1} region using a single function which would describe the whole high-frequency shoulder is not possible in case of lysozyme crystals. The low-frequency Raman spectra of the crystal are composed of the lattice modes overlapping with the internal modes of lysozyme molecule existing because of molecular flexibility and modes of water. Therefore, multiple Gaussian functions were used to reach the best fit of the curve at 150-230 cm^{-1} (Fig. 9b). However, it can be seen in Fig. 10 that $\chi''(\omega)$ of lysozyme crystal is approaching $\chi''(\omega)$ of dry lysozyme at crystal heating that is an evidence of change in the dynamics of H-bond network of water.

Relaxational dynamics of water built in to the lysozyme crystal manifests itself as a QES observable in low-frequency Raman spectra (Fig. 9a). The water of protein crystals can be situated in the close proximity of protein molecule surface forming the so-called hydration shell. The other water fraction, bulk water, fills in the space between protein molecules. The relaxation time, estimated from the width of relaxation component, was found to be ~ $0{,}6 \cdot 10^{-12}$ sec at 298 K. This value is similar to that of bulk water at the same temperature determined by Raman spectroscopy previously [18,44]. The *T*-dependence of intensity of relaxational component is plotted in Fig. 12. It is seen that the intensity is rising monotonically up to 313 K indicating a gradual increase of molecular mobility. Above 313 K the further temperature rise is accompanied by the decrease in QES intensity. According to previous investigation of tetragonal lysozyme crystals with different water contents, there exist pronounced correlation between the water amount in the crystals and intensity of relaxational component [18]: the drier the crystals, the lower the QES. Therefore, the observable decrease in QES intensity above 313 K can be supposed to be due to the start of crystal drying, and, in particular, a removal of water molecules weakly bound to the protein molecules and not belonging to the hydration shell. So, water removal from lysozyme tetragonal crystals occurs here at higher temperature relative to T_{ph} as it has been found by Brillouin light scattering and calorimetric investigations where the onset was detected at ~ 307 K [3-5]. The relaxational motions of protein molecules also contribute to QES of lysozyme crystals. However, this contribution cannot be clearly distinguished due to longer protein relaxation times relative to bulk water.

3.2.2 Analysis of OH-stretching region (3100-4000 cm^{-1})

Since the overwhelming majority of OH groups of lysozyme crystals are a part of water molecules we have investigated OH stretching region laying from 3100 to 3800 cm^{-1} to estimate the change in water content upon crystal heating and to analyse simultaneously the rearrangements in hydrogen bond network possibly accompanying the phase transition. The Raman spectra of tetragonal lysozyme crystal measured at 295 K and 319 K and the spectrum of dry lysozyme powder recorded in the frequency range of CH and OH stretching vibrations are plotted in Fig. 13. The Raman intensity was normalized by the integral intensity of the CH stretching bands, only distinctive of the protein. Consequently, the difference in integral intensities between OH stretching bands for dry and crystalline lysozyme results from the presence of water. Since the intensities of OH bands are strongly modified by crystal heating from 295 K up to 319 K, the further determination and analysis of their *T*-dependences is important.

The difference spectrum of dry lysozyme and crystalline lysozyme is compared with the spectrum of water in Fig. 14a (after normalization by the integral intensity in the region 3000 – 3800 cm^{-1}). The OH stretching spectrum of water is composed of three broad bands determined by a fitting procedure and plotted as dashed lines in Fig. 14a. Band (I) is assigned to the OH stretching vibrations in water molecules within the tetrahedral H-bonded network, band (II) to vibrations in water molecules within a distorted tetrahedral H-bonded network, and band (III) to vibrations of free O-H groups [15]. Fig. 6a shows that the intensity of band (I) in lysozyme crystals is significantly lower than that in the spectrum of water. This indicates that the H-bond network of water in lysozyme crystals is more distorted than in bulk water.

Raman spectrum of the lysozyme crystal collected at 302.5 K and its fitting is depicted in Fig. 14b. Peaks (I) and (II) can be clearly identified in Raman spectrum of lysozyme crystal. A sum of peaks (I) and (II) integral intensities is plotted as a function of temperature in Fig. 15. To plot this dependence, the data analysis was performed using the original Raman spectra. In order to remind the physical meaning of integral intensities of vibrational modes, it is necessary to note that the spectral function $S(\omega)$ is proportional to the imaginary part of susceptibility $\chi''(\omega)$ according to the fluctuation-dissipation theorem [3,30]. Thus, the integral intensity of vibrational modes is proportional to static real susceptibility $\chi'(0)$. The *T*-dependence shown in Fig. 15 exhibits a monotonic decrease with temperature increasing up to ~ 302 K following by the pronounced anomalous rise between 302 and 307 K. We attribute this anomaly to

the phase transition in the crystal. Further temperature increase (above 307 K) leads to a monotonic *T*-dependence of integral intensity. However, at ~ 319 K the value of integral intensity starts to drop significantly due to the crystal drying. Thus, the phase transition in tetragonal lysozyme crystals, which manifests itself as an anomaly in $I_I+I_{II}(T)$ dependence, occurs at temperature lower than the dehydration temperature and is not accompanied by the water removal from the crystals.

To analyse separately temperature changes in intensities of bands (I) and (II) in crystal spectra while crystal heating (Fig. 16), we used spectra normalized by the integral intensity of the CH stretching bands. The data points between 295 K and 302 K were not taken into account because of possible variations caused by normalization procedure. The intensity decrease of band (I) and the concomitant intensity increase of band (II) points out that the distortion of the tetrahedral H-bonded network is enhanced upon heating. It can be seen in Fig. 16 that the increase in H-bond network disordering begins at about T_{ph}. The change in average of intensities with T is fitted by a linear regression and plotted as a dashed line which remains almost constant up to about 313 K. Therefore, it can be concluded that the intensity changes of bands (I) and (II) which occur up to 313 K are not related to the water escape induced by heating.

According to the previous studies of water dynamics in hydrated protein powders or protein solutions, the dynamics of water in hydration shell is slower than in the bulk and water molecules may not be arrange strictly tetrahedraly [18,45,46]. It might lead to the partial distortion in hydrogen network of crystal in comparison with bulk water. At the same time, the fraction of bulk water belonging to the lysozyme crystal undergoes additional disordering of tetrahedral hydrogen network above T_{ph} (Fig. 16). The structural change in the H-bond network of bulk water could be directly related to the phase transition mechanism, for example, play a role of trigger.

4. Conclusions

The here presented Raman scattering study of the phase transition in tetragonal lysozyme crystals has revealed significant changes in high-frequency dynamics of protein. The dynamics of some certain elements of secondary structure, some amino acid residues and disulfide bridges changes upon heating above the phase transition. In particular, hydrogen bonds within α-helixes of lysozyme molecule got stronger and α-helical structures become compressed which probably leads to their disordering in high-temperature phase. The frequency downshift of Tyr residues observed above T_{ph}

most probably indicates the changes in hydrogen bonding between Tyr and water of primary hydrogen shell. This points out at the important role of H-bond network rearrangements near the phase transition temperature.

The analysis of the temperature evolution of Trp, Tyr and Met Raman markers revealed a stable positioning of corresponding amino acid residues in protein molecule. There have been no changes found in hydrophobicity of Trp microenvironment in the whole investigated temperature range. It is evident that no corresponding changes in tertiary structure of lysozyme molecule occur at the phase transition. The changes mainly concern high-frequency dynamics of amino acid residues and S-S bonds: above T_{ph} Trp residues exhibited increased fluctuations around the $C_2{=}C_3{-}C_\beta{-}C_\alpha$ linkage and Met residues underwent an additional extension. At the same time ordering of C–S stretching vibrations and disulfide bridges having ggg conformation demonstrated disordering and stretched vibrational motions.

The bands of CH stretching region also demonstrate pronounced anomalies near 307 K upon heating pointing at strong changes in high-frequency dynamics of protein at the phase transition. The phase transition is accompanied by ordering of symmetric and disordering of the CH_3 stretching vibrations. Opposite, the symmetric CH_2 vibrations become disordered while the asymmetric ones ordered. Also the vibrational modes of CH_3 groups become softer whereas CH_2 modes exhibit hardening above T_{ph}.

The phase transition in tetragonal lysozyme crystals is accompanied also by significant changes in water dynamics. The phase transition has been proved to be independent on crystal dehydration: the loss in water content of the lysozyme crystal was observed at higher temperatures relative to T_{ph}. It has been found that an increase in distortion of tetrahedral hydrogen network of water occurred in the vicinity of T_{ph}. This behavior indicates a disordering process in bulk water which could likely induce disorder within the tertiary structure of protein at the phase transition. The unusual temperature behavior of the lognormal component arising from low-frequency protein dynamics (band 70 cm^{-1} in Fig. 11) suggests that the protein could be strained by reorganization of water molecules.

Acknowledgements

Dr. Anna V. Frontzek (née Svanidze) thanks Université de Lille 1 (F-59655 Villeneuve d'Ascq Cedex, France) for the financial support for her visit to perform the Raman

scattering experiments in the scientific group of Prof. Alain Hédoux. We also thank Dr. Tobias Schrader (JCNS, Forschungszentrum Jülich GmbH, Outstation in Garching) for introducing the molecular graphic program CCP4MG and Dr. Matthias D. Frontzek (Paul Scherrer Institut, Villigen, Switzerland) for useful discussion.

References

[1] K. Harata, T. Akiba, Structural phase transition of monoclinic crystals of hen egg-white lysozyme, Biological Crystallography D62 (2006), 375-382.

[2] I. Dobrianov, S. Kriminski, C.L. Caylor, S.G. Lemay, C. Kimmer, A. Kisselev, K.D. Finkelstein, R.E. Thorne, Dynamic response of tetragonal lysozyme crystals to changes in relative humidity: implications for post-growth crystal treatments, Acta Cryst. D57 (2001) 61-68.

[3] A.V. Svanidze, S.G. Lushnikov, and S. Kojima, Anomalous temperature behavior of hypersonic acoustic phonons in a lysozyme crystal, JETP Letters 84 (2006) 551-555.

[4] A.V. Svanidze, H. Huth, S.G. Lushnikov, S. Kojima, and C. Schick, Phase transition in tetragonal hen egg-white lysozyme crystals, Appl. Phys. Lett. 95 (2009) 263702-1-263702-3.

[5] A.V. Svanidze, H. Huth, S.G. Lushnikov, C. Schick, Study of phase transition in tetragonal lysozyme crystals by AC-nanocalorimetry, Thermochimica Acta 544 (2012) 33-37.

[6] P. Jolles, J. Berthou, High temperature crystallization of lysozyme: an example of phase transition, FEBS Lett. 23 (1972) 21-23; J. Berthou, P. Jolles, A phase transition in protein crystal: the example of hen lysozyme, Biochim. Biophys. Acta 336 (1974) 222-227.

[7] J. Kobayashi, T. Asahi, M. Sakurai, I. Kagomiya, H. Asai, H. Asami, The optical activity of lysozyme crystals, Acta Crystalogr. A54 (1998) 581-590.

[8] W. Rehwald, The study of structural phase transitions by means of ultrasonic experiments, Adv. Phys. 22 (1973) 721-755.

[9] D. Long, The Raman effect: a unified treatment of the theory of Raman scattering by molecules, John Wiley & Sons Inc. (2002).

[10] I.R. Lewis and H. Edwards, Handbook of Raman Spectroscopy, Marcel Dekker Inc. (2001).

[11] D. Naumann, FT-infrared and FT-Raman spectroscopy in biomedical research, Appl. Spectrosc. Rev. 36 (2001) 239-298.

[12] A. Hedoux, Y. Guinet, M. Descamps, The contribution of Raman spectroscopy to the analysis of phase transformations in pharmaceutical compaunds, Internat. J Pharmac. 417 (2011) 17-31.

[13] Y.-S. Li, J.S. Church, Raman spectroscopy in the analysis of food and pharmaceutical nanomaterials, J. Food Drug Anal. 22 (2014) 29-48.

[14] M. Maczka, A. Majchrowski, J. Hanuza and S. Kojima, Temperature-dependent IR and Raman scattering studies of phase transitions in $K_2MgWO_2(PO_4)_2$, J. Phys.: Condens. Matter 25 (2013) 025901-1-8.

[15] A. Lerbret, P. Bordat, F. Affouard, Y. Guinet, A. Hedoux, L.Paccou, D. Prevost, and M. Descamps, Influence of homologous disaccharides on the hydrogen-bond network of water: Complementary Raman scattering experiments and molecular dynamics simulations, Carbohydrate Research 340 (2005) 881-887.

[16] J. Wu, Gaussian analysis of Raman spectroscopy of acetic acid reveals a significant amount of monomers that effectively cooperate with hydrogen bonded linear chains, Phys. Chem. Chem. Phys. 16 (2014) 22458-22461.

[17] V. Kocherbitov, J. Latynis, A.Misiunas, J. Barauskas, and G. Niaura, Hydration of lysozyme studied by Raman specroscopy, J. Phys. Chem. B 117 (2013) 4981-4992.

[18] H. Urabe, Yo. Sugawara, M. Ataka, and A. Rupprecht, Low-frequency Raman spectra of lysozyme crystals and oriented DNA films: dynamics of crystal water, Biophys. J. 74 (1998) 1533-1540.

[19] J. Jacob, C. Krafft, K. Welfle, H. Welfle, and W. Saenger, Melting points of lysozyme and ribonuclease A crystals correlated with protein unfolding: a Raman spectroscopy study, Acta Cryst. D54 (1998) 74-80.

[20] A.B. Kudryavtsev, S.B. Mirov, L.J. DeLucas, C. Nicolete, M. van der Woerd, T.L. Bray and T.T. Basiev, Polarized Raman spectroscopic studies of tetragonal lysozyme single crystals, Acta Cryst. D54 (1998) 1216-1229.

[21] M. Gniadecka, O.F. Nielsen, D.H. Christensen, and H.C. Wulf, Structure of water, proteins, and lipids in intact human skin, hair, and nail, The Journal of Investigative Dermatology 110 (1998) 393-398.

[22] Luis Felipe das Chagas e Silva de Carvalho, Erika Tiemi Sato, Janete Dias Almeida, Herculano da Silva Martinho, Diagnosis of inflammatory lesions by high-wavenumber FT-Raman spectroscopy, Theor. Chem. Acc. 130 (2011) 1221-1229.

[23] Y. Miyazaki, T. Matsuo, and H. Suga, Low-temperature heat capacity and glassy behavior of lysozyme crystal, J. Phys. Chem. B 104 (2000) 8044-8052.

[24] A. Hédoux, R. Ionov, J.-F. Willart, A. Lerbret, F. Affouard, Y. Guinet, M. Descamps, D. Prevost, L. Paccou, and F. Danede, Evidence of a two-stage thermal denaturation process in lysozyme: A Raman scattering and differential scanning calorimetry investigation, J. Chem. Phys. 124 (2006) 014703-014710.

[25] A.V. Svanidze, S.G. Lushnikov, L.A. Shuvalov, Deuterated hen egg-white lysozyme crystals : optimization of the growth conditions and morphology, Crystallography Rep. 50 (2005) 789-795.

[26] http://www.sigmaplot.com/products/peakfit/peakfit.php

[27] G. Bellavia, L. Paccou, S. Achir, Y. Guinet, J. Siepmann, A. Hédoux, Analysis of Bulk and Hydration Water During Thermal Lysozyme Denaturation Using Raman Scattering, Food Biophysics 8 (2013) 170-176.

[28] A. Hédoux, Y. Guinet and L. Paccou, Analysis of the Mechanism of Lysozyme Pressure Denaturation from Raman Spectroscopy Investigations, and Comparison with Thermal Denaturation, J. Phys. Chem. B 115 (2011) 6740-6748.

[29] B. Sjöberg, S. Foley, B. Cardey, M. Enescu, An experimental and theoretical study of the amino acid side chain Raman bands in proteins, Spectrochimica Acta Part A: Molecular and Biomolecular Spectroscopy 128 (2014) 300-311.

[30] S. Lance Cooper, P. Abbamonte, N. Mason, C.S. Snow, M. Kim, H. Barath, J.F. Karpus, C.E. Chialvo, J.P. Reed, Y.-I. Joe, X. Chen, D. Casa, Y. Gan, Raman scattering as a tool for studying complex materials, in: R.P. Prasankumar, A.J. Taylor, Optical techniques for solid-state materials characterization, CRC Press, Boca Raton, Florida, 2011, pp. 193-236.

[31] Z.-Q. Wen, Raman spectroscopy of protein pharmaceuticals, J. Pharmaceut. Sci. 96 (2007) 2861-2878.

[32] C.C.F. Blake, D.F. Koenig, G.A. Mair, A.C.T. North, D.C. Phyllips, V.R. Sarma, Structure of hen egg-white lysozyme. A three dimensional Fourier synthesis at 2 Angstrom resolution, Nature 206 (1965) 757-761; C.C.F. Blake, D.E.P. Grace, L.N. Johnson, S.J. Perkins & D.C. Phillips and R. Cassels, C.M. Dobson, F.M. Poulson & R.J.P. Williams, Physical and chemical properties of lysozyme, in: R. Porter, D. W. Fitzsimons, Ciba Foundation Symposium 60 – Molecular Interactions and Activity in Proteins, Excerpta Medica, Amsterdam, 2008, pp. 137-186.

[33] R.J. Green, I. Hopkinson, and R.A.L. Jones, Unfolding and intermolecular association in globular proteins adsorbed at interfaces, Langmuir 15 (1999) 5102-5110.

[34] G. Gouades, P. Colomban, Raman Spectroscopy of nanomaterials: How spectra relate to disorder, particle size and mechanical properties, Progress in Crystal Growth and Characterization of Materials 53 (2007) 1-56.
[35] H. Takeuchi, Raman structural markers of tryptophan and histidine side chains in proteins, Biopolymers 72 (2003) 305-317.
[36] A.T. Tu, Peptide backbone conformation and microenvironment of protein side chains, in: R.J.H. Clark, R.E. Hester, Spectroscopy of Biological Systems, Wiley, NY, 1986, pp. 47-112.
[37] E. Matrai, M. Gal, G. Keresztury, Interpretation of the CH stretching region of the vibrational spectra of cyclohexane, Spectrochim. Acta A: Molecular Spectroscopy 46 (1990) 29-32.
[38] N.K. Howell, G. Arteaga, S. Nakai, E.C.Y. Li-Chan, Raman spectral analysis in the CH stretching region of proteins and amino acids for investigation of hydrophobic interactions, J. Agric. Food Chem. 47 (1999) 924-933.
[39] L.-Yu Wang, Yu.-H. Zhang, L.-J. Zhao, Raman spectroscopic studies on single supersaturated droplets of sodium and magnesium acetate, J. Phys. Chem. A 109 (2005) 609-614.
[40] R.A. Yadav, M. Kumar, R. Singh, P. Singh, S. Jaiswal, G. Srivastav, R.L. Prasad, Ab initio determination of molecular geometries and vibrational frequencies of CX_3 COOH (X = H, F, Cl, Br), Spectrochim. Acta A 71 (2008) 1565-1570.
[41] G. Giraud, J. Karolin, and K. Wynne, Low-frequency modes of peptides and globular proteins in solution observed by ultrafast OHD-RIKES Spectroscopy, Biophys. J. 85 (2003) 1903-1913.
[42] T. Nakayama, Low-Energy Excitations in Water: A Simple-Model Analysis, Phys. Rev. Lett. 80 (1998) 1244-1247.
[43] J.A. Padro, J. Marti, An interpretation of the low-frequency spectrum of liquid water. J. Chem. Phys. 118 (2003) 452-453.
[44] K. Mizoguchi, Y. Hori, Y. Tominaga, Study on Dynamical Structure in Water and Heavy Water by Low-Frequency Raman Spectroscopy, J. Chem. Phys. 97 (1992) 1961-1968.
[45] W. Doster, The protein-solvent glass transition, Biochim. Biophys. Acta 1804 (2010) 3-14.
[46] W. Doster, The two-step scenario of the protein dynamical transition, Journal of Non-Crystaline Solids 357 (2011) 622-628.

Table 1

The list of bands observed in Raman spectra of tetragonal lysozyme crystal and their assignment according to [15,17,18]. ν_{sym} and ν_{as} are symmetric and asymmetric stretching vibrations, respectively.

Band Frequency (cm^{-1})	Assignment to functional group
fingerprint region	
507	ggg disulfide bridges
525	ggt disulfide bridges
694	Met
759	Trp (W18 mode)
835	Tyr (Fermi doublet)
858	Tyr (Fermi doublet)
899	main chain vibration $\nu(C_\alpha\text{-}C)$
930	main chain vibration $\nu(C_\alpha\text{-}C)$
1003	Phe (F1 mode)
1010	Trp (W16 mode)
1176	Tyr (Y9a mode)
1194	Tyr (combination of Y13 and Y6a modes)
1209	Tyr, Phe (F7a mode)
1231	Amide III
1258	Amide III
1340	Trp (Fermi doublet)
1262	Trp (Fermy doublet)
1552	Trp
1613	Tyr
1659	Amide I
C-H stretching region	
2875	$\nu_{sym}(CH_3)$
2907	$\nu_{sym}(CH_2)$
2933	$\nu_{as}(CH_2)$
2964	$\nu_{as}(CH_3)$
3059	$\nu(CH)$

Figures

Figure 1

Raman scattering geometry utilized in experiments with lysozyme crystals. k_i and E_i are wave vector and polarization of incident light, k_s and E_s are wave vector and polarization of scattered light.

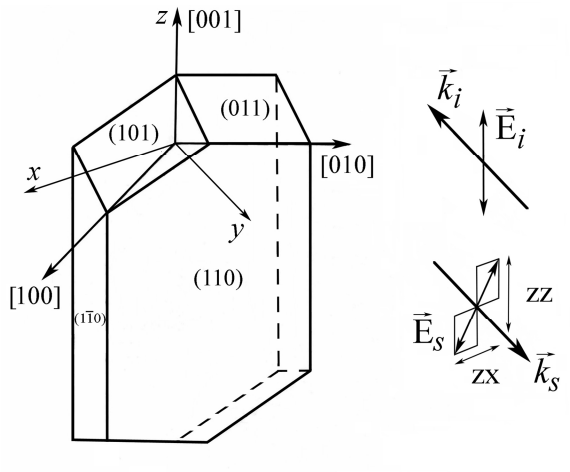

Figure 2

Raman spectra of the tetragonal lysozyme crystal measured in frequency range of fingerprint region at different temperatures: 301 K (black line), 307 K (red line), 310 K (blue line), 314 K (yellow line) and 317 K (green line). The assignment of some peaks in Raman spectra to the vibrations of certain functional groups or structural elements of lysozyme molecule is shown in the Figure. The insert depicts the temperature dependence of relative integral intensity (Raman spectra were normalized by the total integral intensity) for Trp band located at 759 cm^{-1}. The color of the spectrum and the color of experimental points in the insert are the same for the same temperature. Dashed line shows that the black spectrum corresponds to the temperature of 301 K.

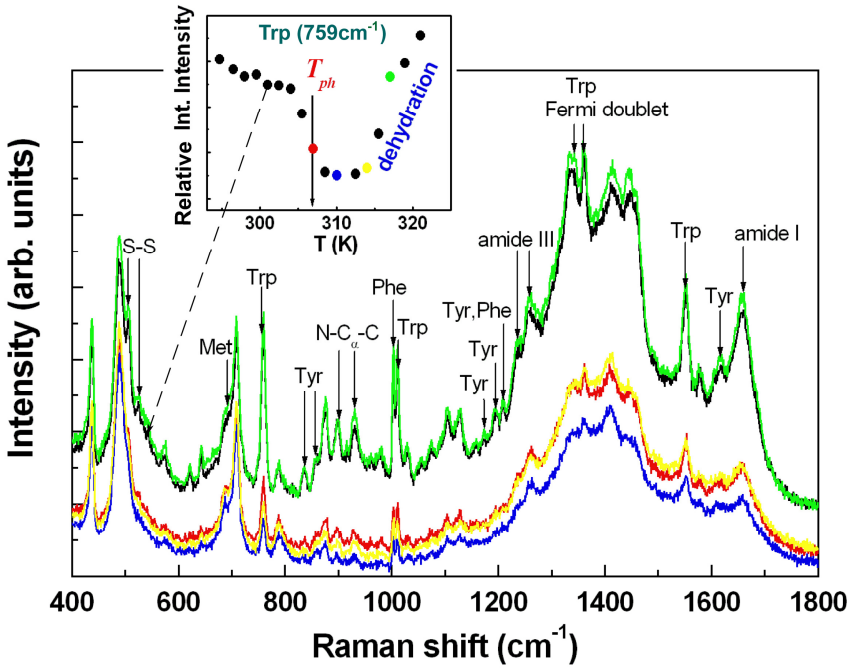

Figure 3

Temperature evolution of vibrational modes of tetragonal lysozyme crystal: (a) Raman spectrum of the crystal in the vicinity of amide I band and its fitting; (b) temperature dependence of frequency and bandwidth of amide I band; (c) Raman spectrum in the region of amide-III bands and their fitting; (d) temperature dependencies of Raman shifts of amide-III bands located at 1235 and 1259 cm^{-1}; (e) Raman spectrum in the region of main chain stretching vibrations N-C_{α}-C and its fitting; (f) temperature dependencies of Raman shifts of bands originating from main chain stretching vibrations. All presented Raman spectra were measured at 298 K. The spectra obtained in Raman scattering experiment are plotted in panels (a), (c) and (e) by gray circles. The final function used for spectra fitting and fitting of certain bands by Lorentzians or Gaussians are shown by solid and dashed black lines, respectively.

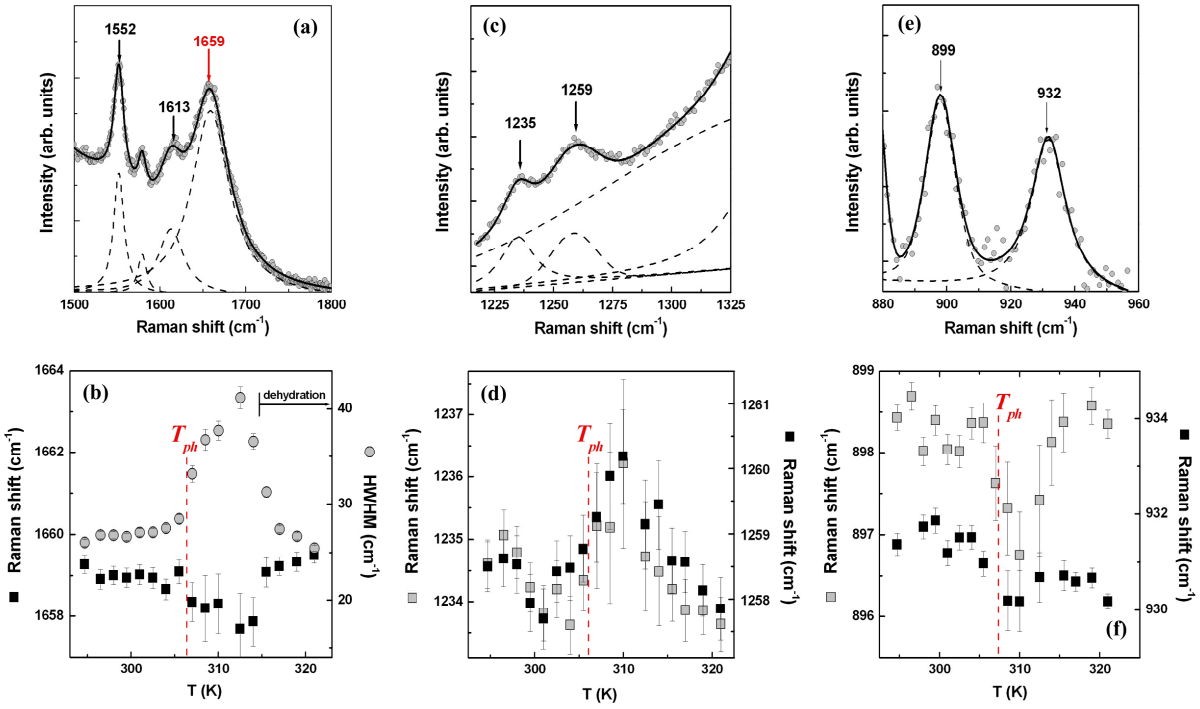

Figure 4

Temperature dependences of frequency and bandwidth (HWHM is a half-width at half-maximum) of 1552 cm^{-1} band arising from C_2=C_3 stretching vibrations of Trp indole rings. The values of Raman shift are shown by black squares, the values of HWHM – by gray circles. The inserts in the figure show locations of Trp residues in lysozyme molecule and structural formula of Trp residue.

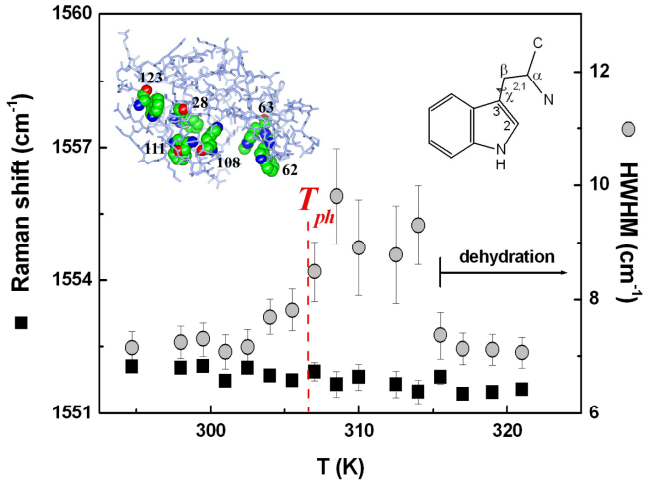

Figure 5

Temperature dependences of frequency and bandwidth (HWHM is a half-width at half-maximum) of 1613 cm^{-1} band originating from C-C stretching vibrations within the aromatic ring of Tyr groups. The values of Raman shift are shown by black squares, the values of HWHM – by gray circles. The insert in the figure shows locations of Tyr residues in lysozyme molecule.

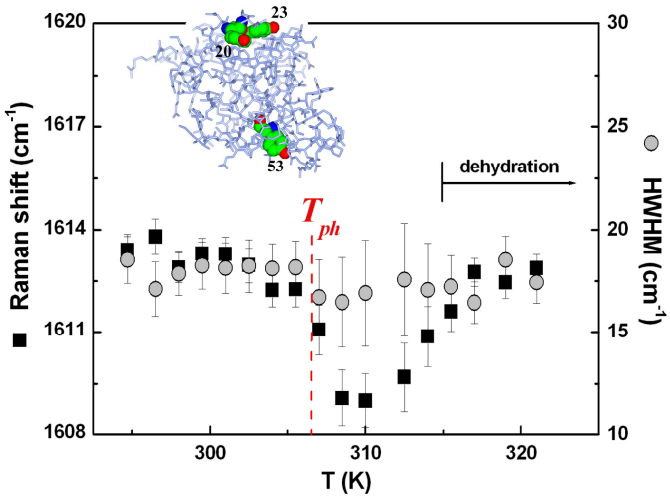

Figure 6

Temperature evolution of 694 cm^{-1} band originating from C–S stretching vibrations of Met residues of lysozyme molecule: (a) Raman spectrum in the vicinity of the band and its fitting, the insert shows locations of Met residues in lysozyme molecule; (b) temperature dependencies of frequency and bandwidth (HWHM is a half-width at half-maximum) of the band. The values of Raman shift are shown by black squares, the values of HWHM – by gray circles.

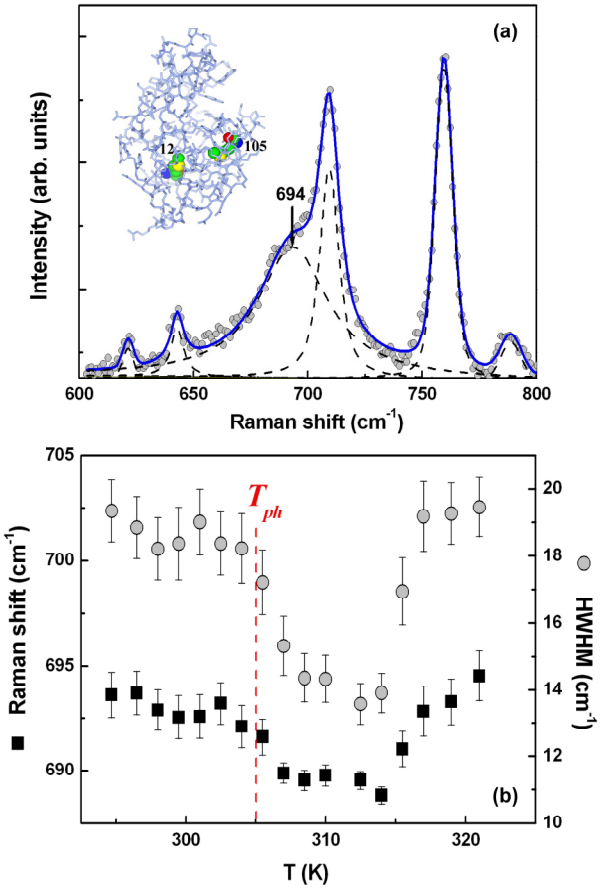

Figure 7

The Raman spectrum of tetragonal lysozyme crystal measured at 295 K (gray circles) with the result of its fitting (blue line) by Lorentzians (the band located at 2964 cm^{-1}) and Gaussians (the other 4 bands in CH-stretching region).

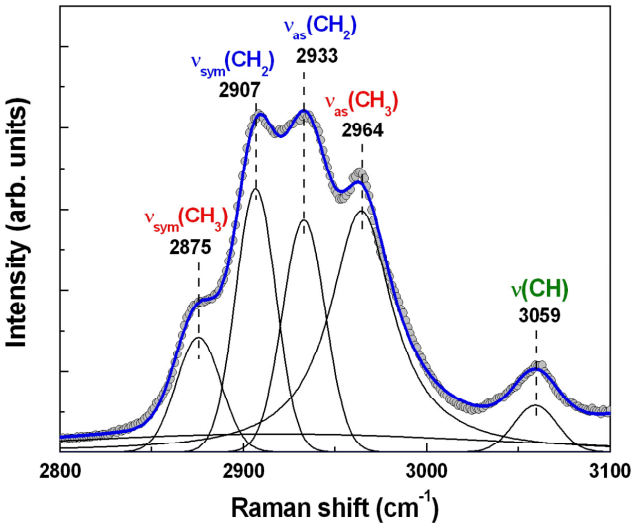

Figure 8

Temperature dependencies of frequencies and bandwidth of bands located in CH-stretching region of lysozyme crystal Raman spectra at 2875, 2907, 2933 and 2964 cm^{-1}.

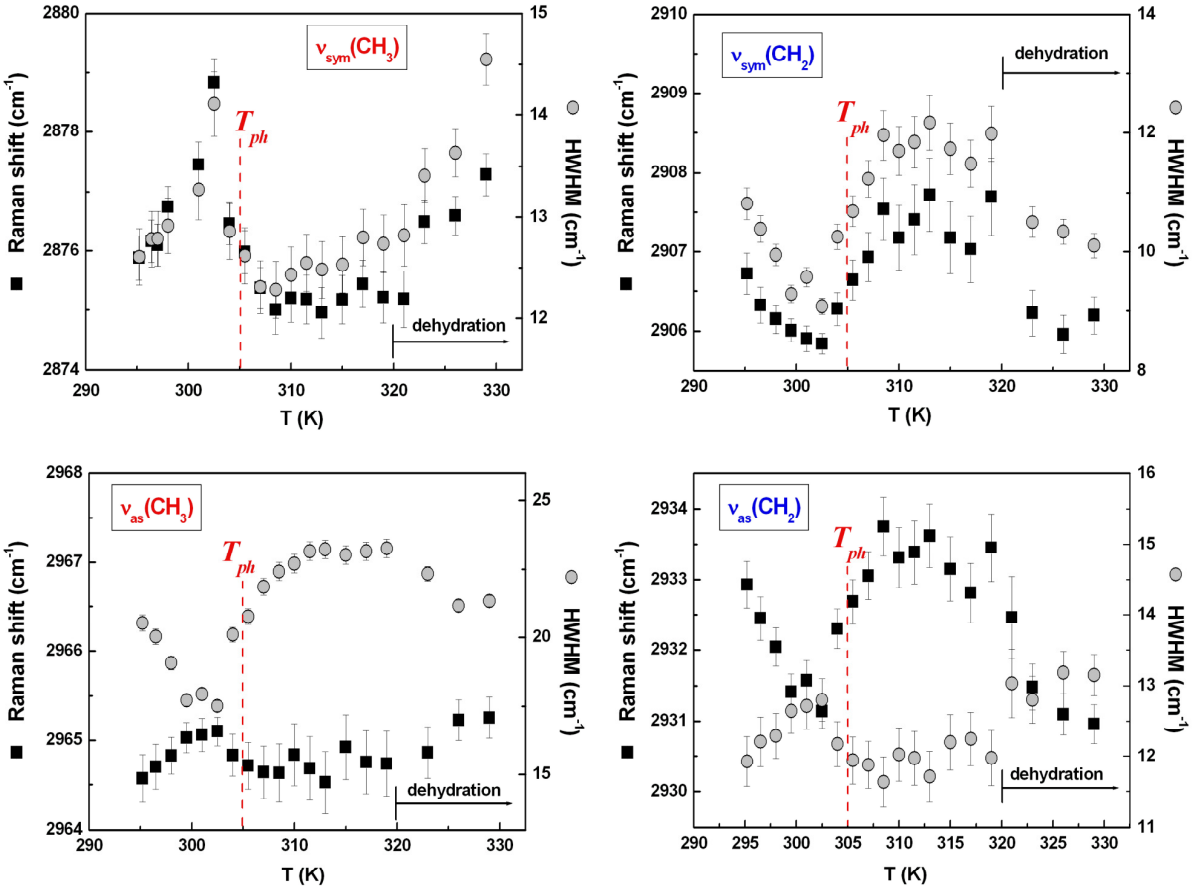

Figure 9

(a) Low-frequency Raman spectrum of tetragonal lysozyme crystal and its fitting; (b) $\chi''(\omega)$ spectrum of tetragonal lysozyme crystal obtained from Raman spectrum represented in panel (a).

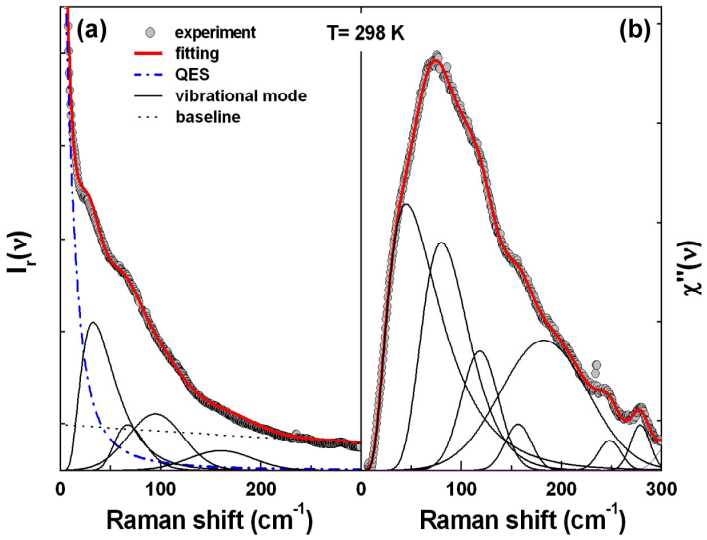

Figure 10

Low-frequency Raman spectra of dry lysozyme (green line), 20% lysozyme aqueous solution (blue line) and lysozyme crystal measured at room temperature T_{room} (red line) and 310 K (black line). The data for dry lysozyme and lysozyme solution were taken from paper A. Hédoux et al. [22].

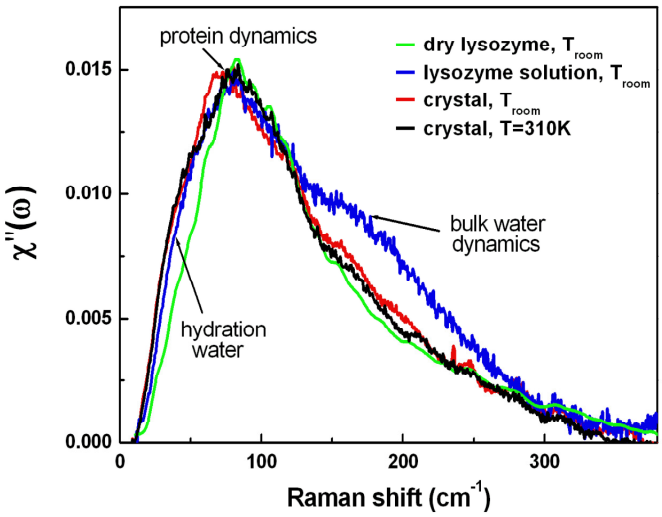

Figure 11

Temperature dependence of Raman shift maximum for the band in low-frequency region arising from protein dynamics.

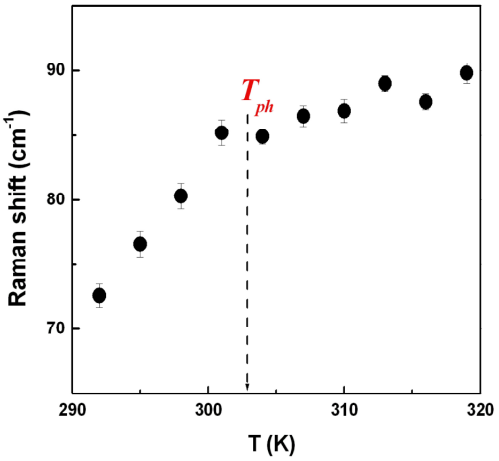

Figure 12

Temperature dependence of QES intensity obtained by the analysis of low-frequency Raman spectra of the tetragonal lysozyme crystal.

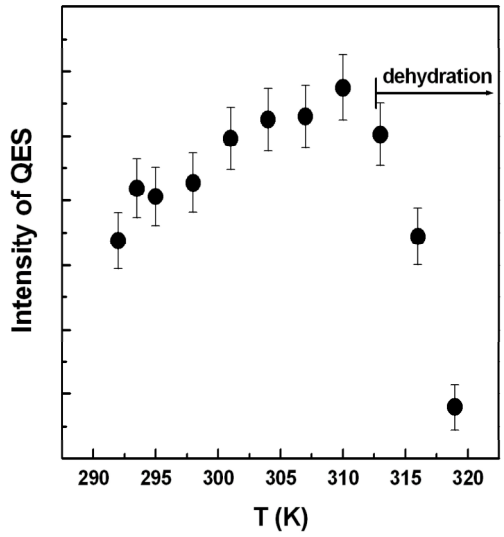

Figure 13

Raman spectra in the frequency range of CH and OH stretching vibrations obtained from the tetragonal lysozyme crystal at 295 K (green line) and 319 K (red line) and the spectrum of dry lysozyme powder measured at room temperature (blue line).

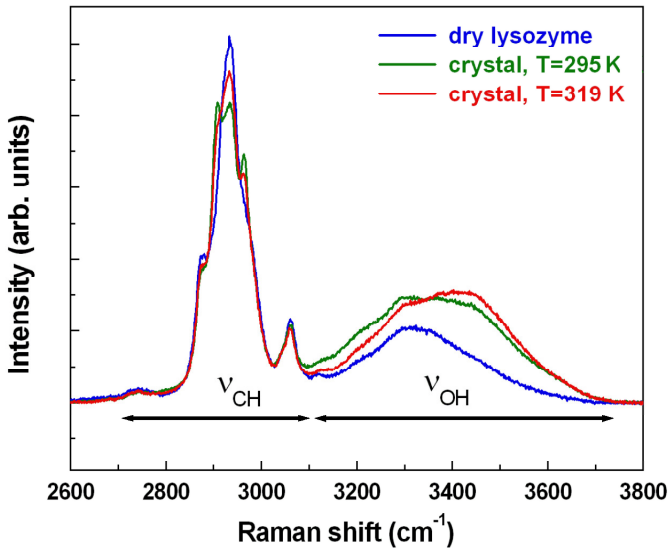

Figure 14

(a) The comparison of the differential Raman spectrum obtained by subtraction of dry lysozyme spectrum from the spectrum of tetragonal lysozyme crystal measured at 295 K (blue line) with the Raman spectrum of pure water (black line). The peaks (I), (II) and (III) are the result of water spectrum fitting. (b) Raman spectrum of tetragonal lysozyme crystal measured at 295 K and the results of its fitting.

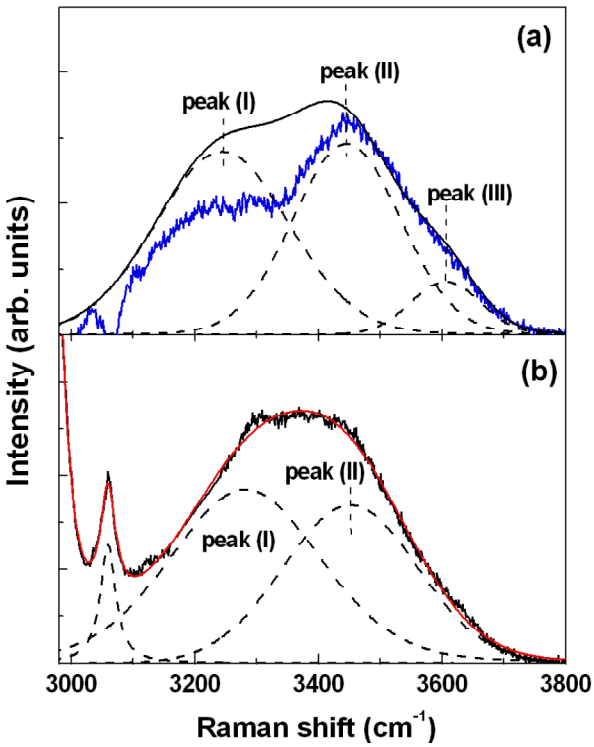

Figure 15

The sum of integral intensities of OH stretching bands (peak (I) and peak (II)) of the tetragonal lysozyme crystal plotted as a function of temperature.

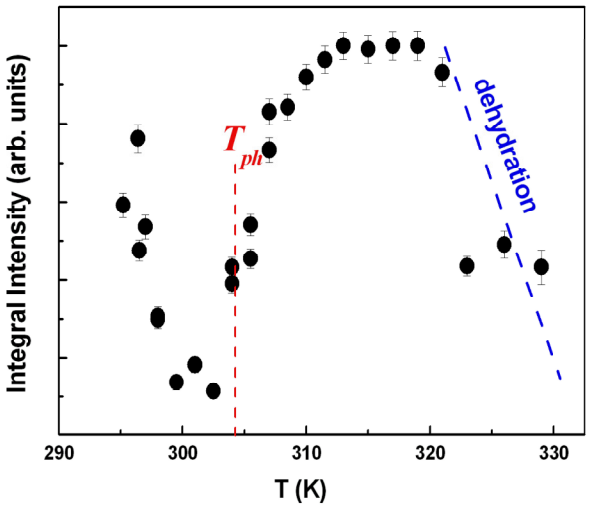

Figure 16

Temperature dependences of relative intensities for peaks (I) (black triangles) and (II) (black circles) and their average $(I_I+I_{II})/2$ (gray squares).